THE ASIAN SYMPOSIUM ON COMPUTATIONAL HEAT TRANSFER AND FLUID FLOW - 2011, 22−26 SEPTEMBER 2011, KYOTO, JAPAN

Paper ID: 040

Numerical analysis of the influence of thermal boundary condition and surface emissivity on the flow and heat transfer in turbulent buoyancy driven flow

Draco Aluya Iyi[1], Reaz Hasan[2], Roger Penlington[3]

School of Computing, Engineering & Information Sciences,

Northumbria University, Newcastle upon Tyne, NE1 8ST, United Kingdom

*corresponding author, E-mail: Reaz.hasan@unn.ac.uk

Abstract

Numerical analysis of coupled radiation and natural convection is reported for a two-dimensional air-filled square cavity whose vertical surfaces are maintained at constant differential temperatures while the horizontal surfaces are treated for three different boundary situations. The buoyancy driven flow considered in this work has a typical Rayleigh number of 1.5 x 10^9. The effect of radiation has been found to be very significant even for the moderate temperature difference of 40^0c between the hot and the cold walls. As expected, heat transfer is found to increase with a higher value of surface emissivity.

.

1. Introduction

Natural convection in air filled cavities had been the subject of extensive research for the last two decades due to its relevance in many practical flows such as heat transfer in buildings [1], electronic and other cooling processes [2-3], etc. One particular configuration which has attracted significant attention from researchers is the square configuration with differentially heated vertical surfaces [4-9]. This is due to the fact that experimental set up is relatively easier for this geometry and hence detailed and sensitive data can be collected. Following on, numerical scientists had also been quick to respond to the experimental literature by conducting validation and exploratory studies on this very topic. The interest seems to be ongoing because more challenging situations are emerging with time [10-11]. In the case of a square cavity of dimension L, shown in Fig.1, the natural convection heat transfer from hot to cold wall is characterized by the formation of a slow moving vortex. The fluid particles move up along the hot vertical wall (temperature T_h) by absorbing heat from the 'source', and then it flows downward along the cold wall gradually losing the heat to the cold surface (temperature T_c) which may be termed as the 'sink'. Depending on the Rayleigh number the flow can be turbulent or laminar. In most cases the flow is found to be dominated by turbulence near the walls for Rayleigh number greater than 1.2×10^9 [6]. The Rayleigh number is defined as

$$R_a = \frac{g\beta\Delta TL^3}{\mu\alpha} \qquad (1)$$

Where, β is coefficient of thermal expansion; $\Delta T = T_h - T_c$; g is the acceleration due to gravity, μ and α represent the density, viscosity and the thermal diffusivity of the fluid respectively.

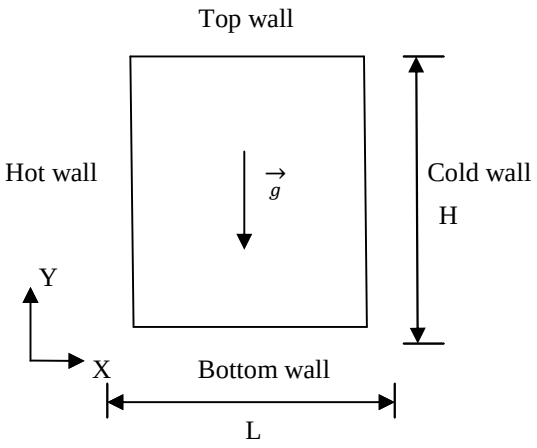

Figure 1: Geometry and the coordinates

From numerical analysis point of view, the accuracy of computations is affected by the choice of grids, the turbulence models and other numerical issues and these have been the major concern for the numerical scientists [1, 12-13]. One apparently obvious point which causes differences in results is due to the choice of thermal boundary conditions for the walls. While the vertical surfaces have well defined boundaries namely, isothermal walls, the boundary conditions for the horizontal walls are highly variable. The most common one that the numerical codes employ is adiabatic condition. However, due to practical problems this is not usually achievable. In this paper, we investigate the two dimensional natural convection for a square cavity with particular attention given on the choice of boundary condition for the horizontal walls. Another aspect which is focused in this work is the importance of radiation for this simple geometry. By changing the surface emissivity's value we had been able to

quantify the effects of radiation on the overall heat transfer. This issue may be particularly relevant for situations where high emissivity surface properties are encountered.

2. Numerical method

Calculations were carried out using the FLUENT commercial package [14]. For discretisation of convection terms, second order upwind scheme has been followed for all the governing equations. While isothermal boundary conditions have been selected for vertical walls ($T_h = 50^0$c and $T_c = 10^0$c), three different thermal boundary conditions have been chosen for the horizontal walls. These are abbreviated as ATP, LTP and ETP as explained below.

ATP represents Adiabatic Temperature Profile i.e., the walls are perfectly insulated; LTP is a Linear Temperature Profile and corresponds to a perfect conduction and ETP represents Experimental Temperature Profile. The mathematical meanings are shown in Table 1 below.

Table 1: The three thermal boundary conditions

Boundary conditions	Temperature functions
ATP	$\partial T/\partial x = 0$
LTP	$T_L = T_c + \Delta T(x+1)$
ETP	$T_E = T_c + \Delta T(T^*)$

The experimental temperature profile (ETP) is a best-fit polynomial based on the experimental data of Tian and Karayiannis (2000) [6], and T^* is defined by the following polynomial and the coefficients are given in Table 2.

$$T^* = a\left(\frac{x}{L}\right)^4 + b\left(\frac{x}{L}\right)^3 + c\left(\frac{x}{L}\right)^2 + d\left(\frac{x}{L}\right) + e \qquad (2)$$

Table 2: Coefficients for the polynomial of Equation (2)

Walls	a	b	c	d	e
Top	-2.458	1.686	1.211	-1.440	1
Bottom	2.458	-8.146	8.477	-3.789	1

The above boundary conditions were implemented with a user subroutine in FLUENT. The fluid is initially motionless and at a uniform temperature equal to the average temperature of the vertical walls. Thermo-physical properties of dry-air are estimated at this mean temperature of the isothermal vertical walls.

Based on another preliminary study to ascertain the effect of turbulence model, a detailed investigation was carried out. The model chosen for this study was the low Reynolds number model of Yang-Shih [15], as this was found to have shown the best agreement. Some details of the results on the turbulence model sensitivity are shown in the following section. Systematic investigation was carried out using various grid densities and the final calculations were found to be grid independent. The grid density was 220 x 220 with a non-uniform spacing and the typical y^+ value was less than 0.5.

3. Results and discussion

3.1. Choice of turbulence model

It is well known that turbulence models play an important role in the predictions of fluid flows. A total of six eddy-viscosity (EVM) turbulence models have been tried. The reason that we restricted ourselves to the EVM is due to the fact that other advanced turbulence modelling such as LES is still very demanding from computation point of view and it is unlikely that it can be applied to practical flows. Hence it is much more important to scrutinise the models that are likely to be used from the viewpoint of practitioners. Figs. 2 and 3 show the typical mean quantity profiles predicted by various turbulence models. A careful look at the plots reveal that while the core region had been predicted well by most of the models, the situation is very different for the near wall region. For both cases (velocity and temperature), it is clear that the Yang-Shi model (ref) return the best results. Hence this model has been used for all the calculations reported in this work.

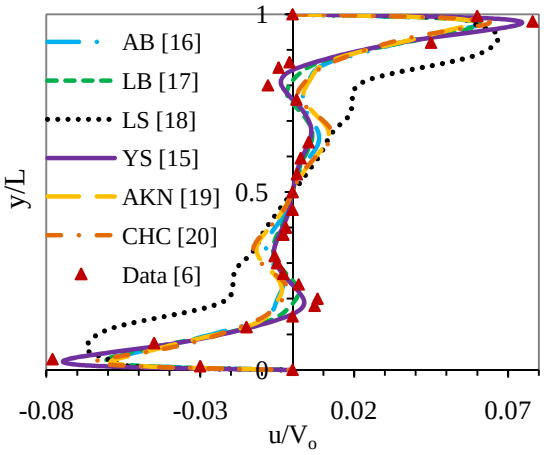

Figure 2: Horizontal component of mean velocity at x/L=0.5

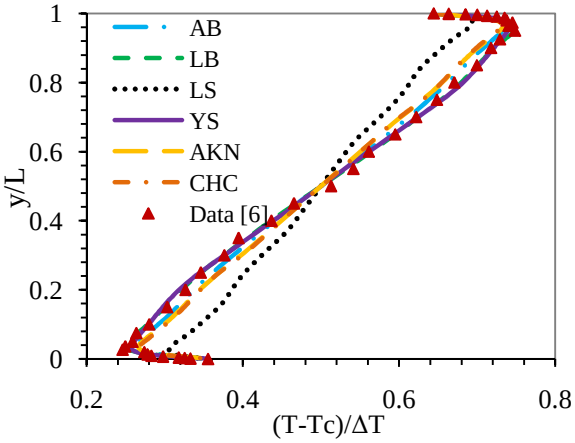

Figure 3: Non-dimensional mean temperature at x/L=0.5

3.2. Effect of boundary condition

References Fig. 4 shows the stream function plots for the three different boundary conditions. The flow field is characterized by a stable stratified flow with a core region in the middle. However, the adiabatic temperature profile on the horizontal walls shows more uniform velocity as the core region is rather squeezed towards the centre plane. On the other hand the linear temperature profile and the experimental temperature profile boundary conditions display very similar stream functions with the former showing higher velocity gradient near the vertical walls.

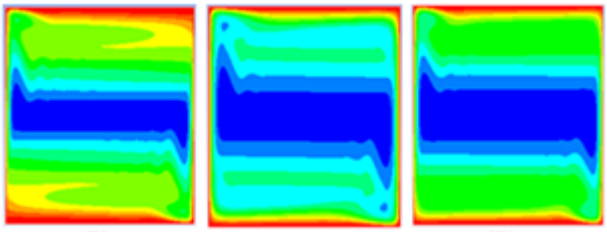

Figure 4: Stream function plots for three boundary conditions.

This observation is in line with the mean horizontal velocity component u, prediction as shown in Fig. 5. V_0 is the buoyancy velocity defined in equation 3.

$$V_0 = \sqrt{g\beta L\Delta T} = 1 \text{ (m/s)} \qquad (3)$$

The correctness of the ETP boundary condition can be clearly seen from this plot. It can be argued that the ETP profiles display maximum discrepancies at a distance of one quarter from the walls, but it should be recognised that the magnitude of the velocity in this region is very small. As a matter of interest, the numerical result of Nicholas [5], is also included in the figure which clearly demonstrates the improvement in our calculations. A similar set of results is presented in Fig. 6, where we compare the vertical component of the velocity v, along the mid-height of the square cavity.

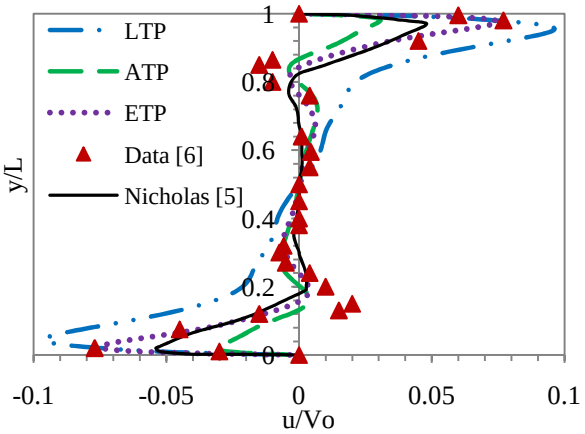

Figure 5: Mean horizontal component of velocity at x/L=0.5

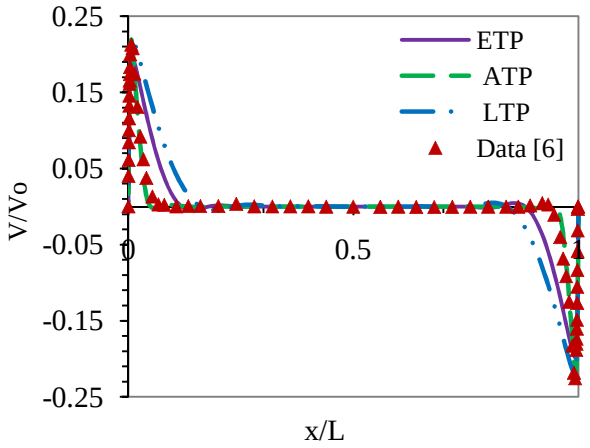

Figure 6: Mean vertical component of velocity at y/L=0.5

Fig.7a-c show the turbulence intensity comparison for the three cases for three locations y/L=0.125, 0.25 and 0.5. It can be seen from y/L=0.5 location, that the ETP can predict the maximum turbulence near the walls more accurately than the other two boundary conditions. One limitation is that the asymmetry, as evidenced in the experimental data, in the maximum magnitude of turbulence intensity is not well predicted by any of the boundary conditions. However, the turbulence intensity asymmetry is better predicted at two other locations.

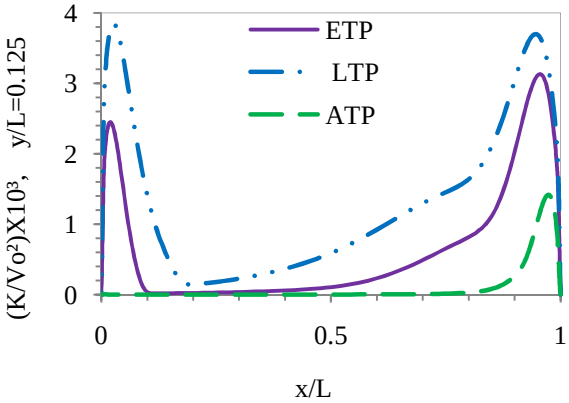

Figures 7a: Comparison with turbulence intensity profiles for y/L=0.5

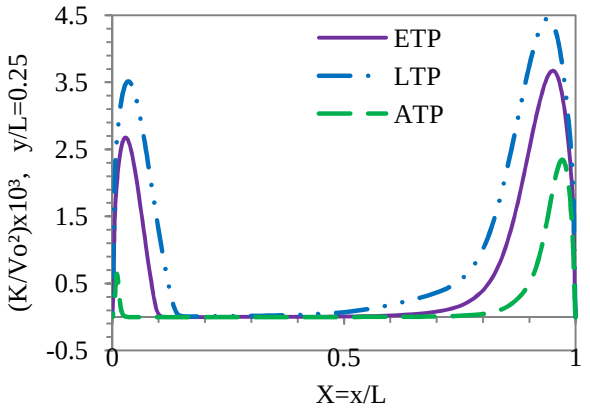

Figures 7b: Comparison with turbulence intensity profiles for y/L= 0.25

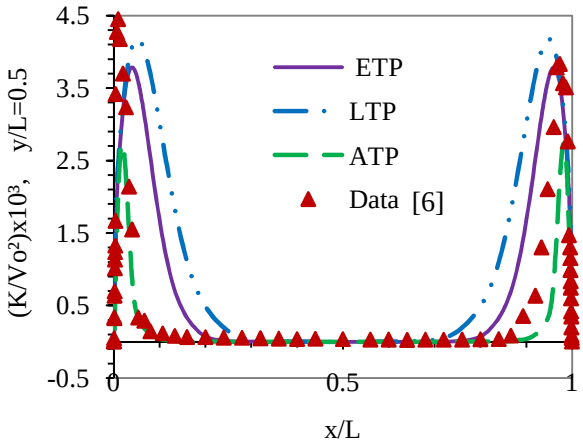

Figures 7c: Comparison with turbulence intensity profiles for y/L= 0.125

The turbulence intensity contours shown in Fig. 8 demonstrates that the shear layer in the case of ATP is concentrated only in the two diagonally opposite corners whereas for the other two boundary conditions, very similar contours can be observed. In all cases, the flow field is seen to be dominated by turbulence only in the near wall regions and the core area is essentially a bulk mean flow with a rather stagnating condition. This observation further highlights the importance of using a low-Re model.

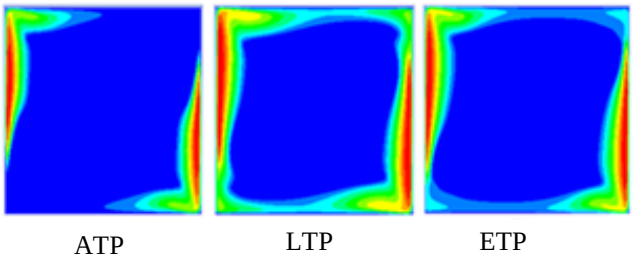

Figure 8: Contours of turbulence intensity for three boundary conditions

The plots related to the heat transfer are shown in Figs. 9-13. For the mean temperature profile (Fig. 9) along the mid-width (x/L=0.5) of the cavity, the ETP shows the best agreement while the ATP over- or under-predict the temperature at the passive horizontal walls by as much as 200%. The importance of an appropriate boundary condition and the choice of a suitable low-Re turbulence model are hence further emphasized by these plots. In fact, the temperature distribution is the most critical mean quantity due to the fact that this may be interpreted as both 'cause' and 'effect' and vice versa. The flow develops due to the buoyancy which is directly dependent on temperature and at the same time temperature is also affected by the flow field.

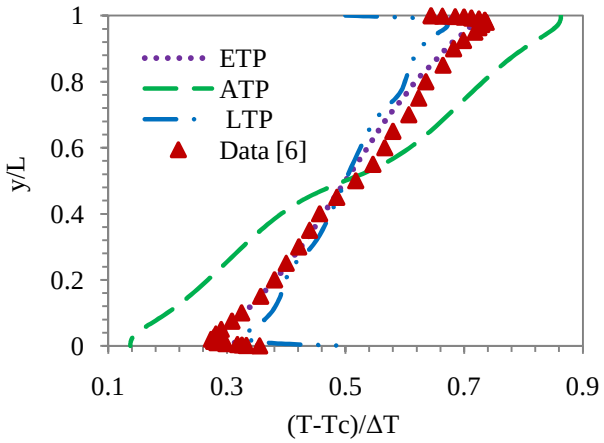

Figure 9: Mean temperature at x/L=0.5

Figs. 10-13 present the local Nusselt numbers defined by $Nu = {}^{q_i L}/_{K\Delta T}$, where q_i represents the local heat flux evaluated at each node and k is the thermal conductivity. Comparisons with experimental and/or numerical results are also included wherever possible. Although there are discrepancies between the various predictions, overall, the ETP boundary conditions appear to be better. The ATP boundary condition fails to mimic the qualitative trends observed in experiments.

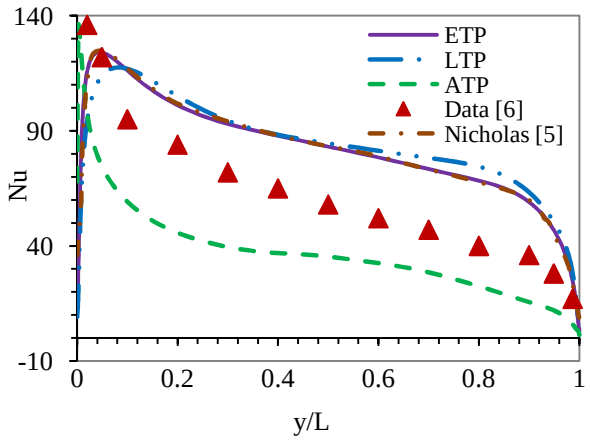

Figure 10: Local Nusselt number along the hot wall

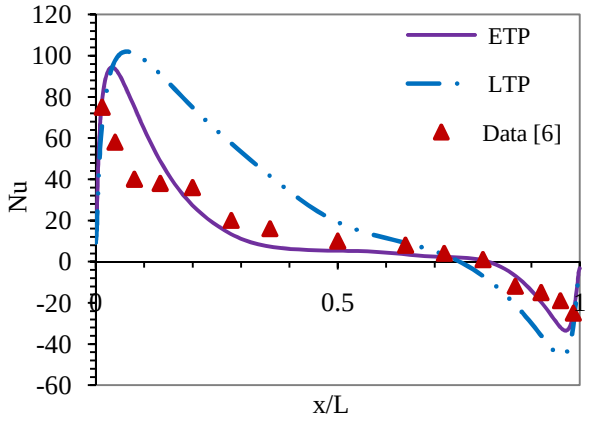

Figure 11: Local Nusselt number along the bottom wall

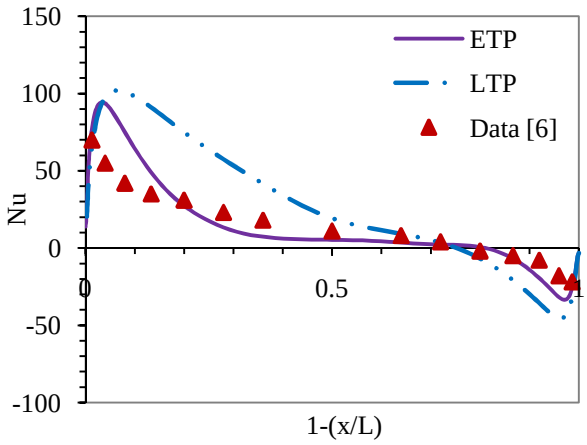

Figure 12: Local Nusselt number along the top wall

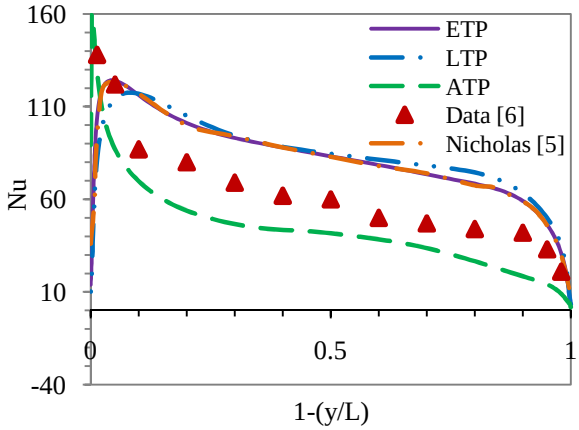

Figure 13: Local Nusselt number along the cold wall

Finally, the predicted values of the average Nusselt numbers are shown in Table.2. Again, the values returned by the ETP is very close (less than 1% difference) to the experimental values for the active wall and the ATP is furthest.

Table 3: Comparison of average Nusselt numbers

Average Nusselt Number				
Surfaces	ETP	LTP	ATP	DATA [5]
Cold	62.75	64.28	52.80	62.60
Hot	62.59	64.28	52.80	62.90

3.3. Influence of surface emissivity

Further calculations were carried out for the above flow geometry to explore the influence of surface emissivity on the heat transfer. The wall boundary conditions for the vertical walls were isothermal and the horizontal walls were specified the ETP boundary condition as described before. The surface emissivities were varied. To model the radiation the S2S radiation model was adopted from the FLUENT. The reason for the choice of the S2S model was that it is found to give better results. Different four emissivity values were specified such as $\varepsilon_0 = 0$, $\varepsilon_1 = 0.2$, $\varepsilon_2 = 0.5$ and $\varepsilon_3 = 0.7$. Figure 14-17 show the local Nusselt number for the walls as the emissivity is changed, with average values shown in Table 4. Therefore, changes in the surface radiation enhances the heat transfer process, since an increase in surface emissivity values leads to corresponding increase of the local Nusselt number.

Table 4: Average Nusselt number

Average Nusselt Number				
Surfaces	ε_0	ε_1	ε_2	ε_3
Bottom	10.31	10.57	20.75	37.01
Cold	56.16	65.55	56.16	56.16
Hot	56.16	80.75	94.33	113.6
Top	10.31	1.80	16.92	20.35

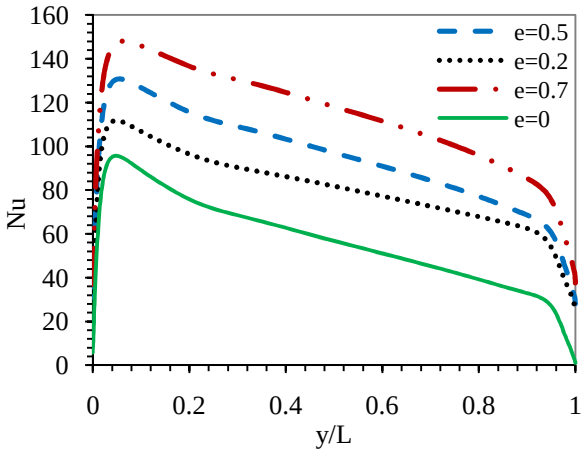

Figure 14: Local Nusselt number along the hot wall

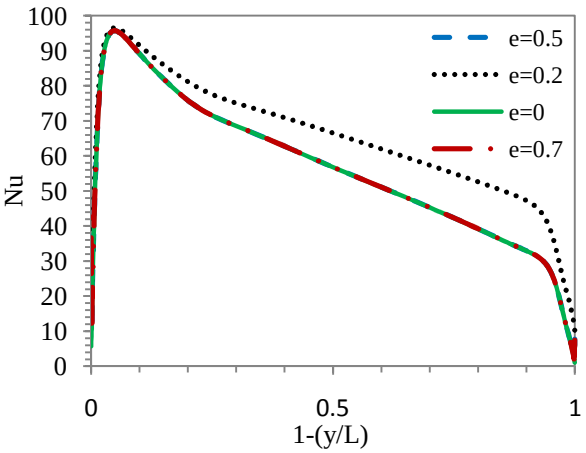

Figure 15: Local Nusselt number along the cold wall

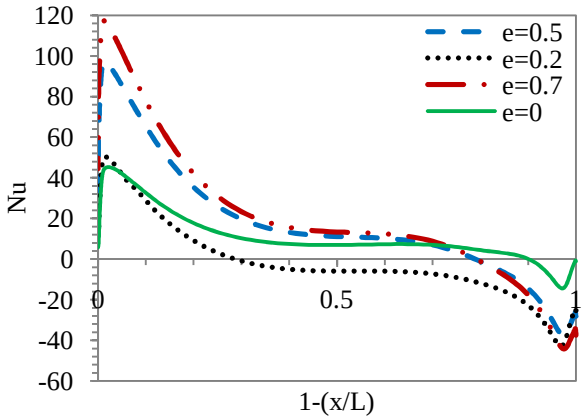

Figure 16: Local Nusselt number along the top wall

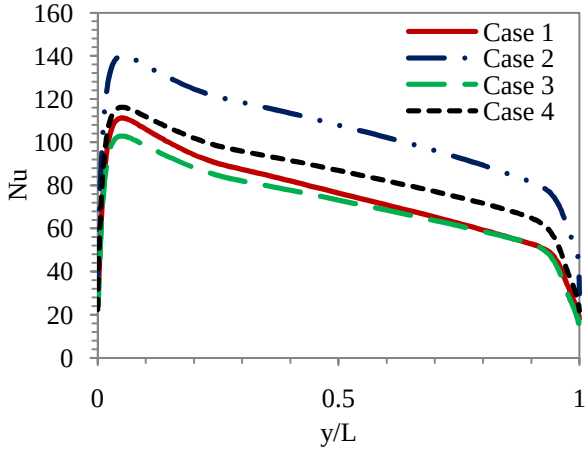

Figure 18: Local Nusselt number along the hot wall

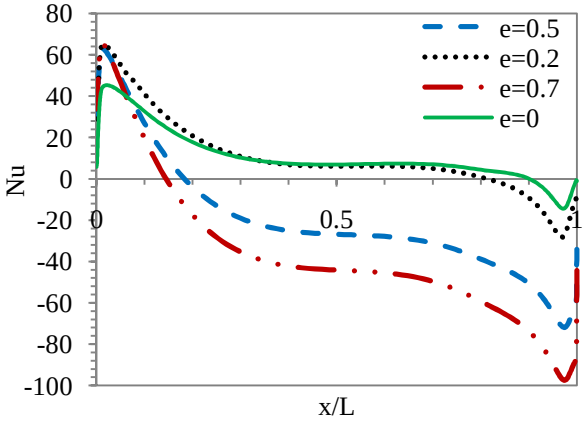

Figure 17: Local Nusselt number along the bottom wall

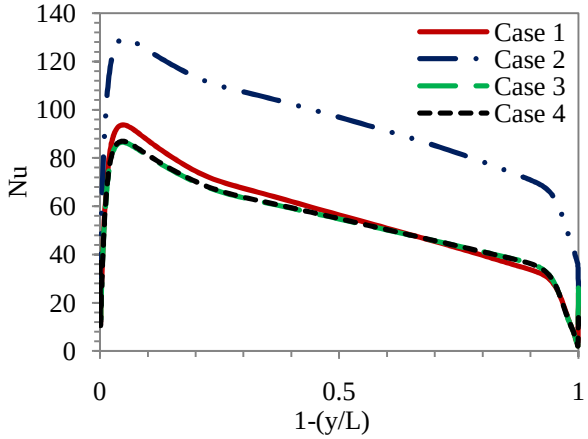

Figure 19: Local Nusselt number along the cold wall

Further exploratory investigation was carried out by changing the emissivity values in pairs for four different cases as shown in Table 5. The variations of local Nusselt number are plotted in Figures 18-21. It can be seen that the local Nusselt number changes with the changes in the surface emissivity. In addition, the value of surface emissivity for the passive and hot walls has a significant effect on the heat transfer within the cavity.

Table 5: Wall emissivity for all case

Cases	Top wall	Bottom wall	Cold wall	Hot wall
1	0.2	0.5	0.5	0.2
2	0.2	0.2	0.5	0.5
3	0.5	0.5	0.2	0.2
4	0.5	0.2	0.2	0.5

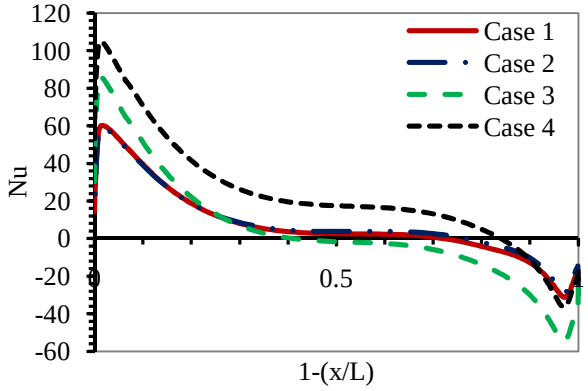

Figure 20: Local Nusselt number along the top wall

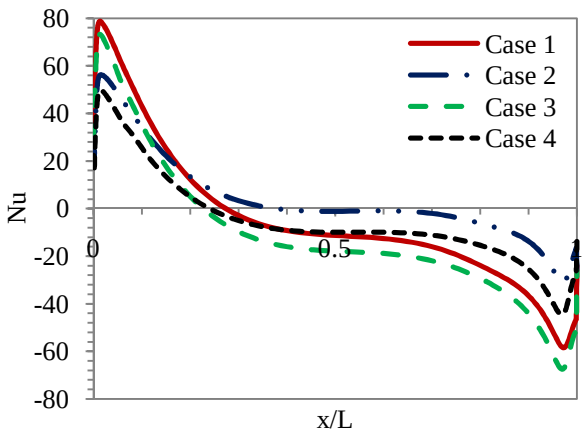

Figure 21: Local Nusselt number along the Bottom wall

4. Conclusions

The work presented in this paper highlights the fact that turbulent natural convection flow is very sensitive to the appropriate choice of boundary specification. At the same time since the flow is dominated by turbulence mainly near the walls, it is also important to resolve the flow variables in this region very carefully. A detailed understanding of the performance of EVM is essential. The numerical results for the surface emissivity used in this study cause changes in the conditions of the energy equation, which has a great effect on the heat transfer and influences the weak natural convection flows.

Acknowledgements

My appreciation goes to my supervisors, Dr. Reaz Hasan and Dr. Roger Penlington for all the critical discussions, technical assistance and generally maintaining an excellent research motivation. The work presented in this paper forms a part of a larger study on low speed turbulent natural convection heat and mass transfer which belongs to the design and manufacturing research group (DMRG) at Northumbria University.

References

[1] W. Chen, W. Liu, Numerical and experimental analysis of convection heat transfer in passive solar heating room with greenhouse and heat storage, Solar Energy 76: 623–633, 2004.

[2] S. Kadem, A. Lachemet, R. Younsi, D. Kocaefe, 3d-Transient modeling of heat and mass transfer during heat treatment of wood, *International Communications in Heat and Mass Transfer* 38*: 717-722*, 2010.

[3] O. Laguerre, S. Ben Amara, D. Flick, Experimental study of heat transfer by natural convection in a closed cavity: Application in a domestic refrigerator. *Journal of Food Engineering*, 70: 523–537, 2005.

[4] B. Calcagni, F. Marsili, M. Paroncini, Natural convective heat transfer in square enclosures heated from below. *Applied Thermal Engineering* 25: 2522–2531, 2005.

[5] D. Nicholas, Jr. Francis, Characterization of Fuego for Laminar and Turbulent Natural Convection Heat Transfer, in Thermal and Reactive Processes Department, Sandia National Laboratories: Albuquerque, 2005.

[6] S.Y. Tian, T.G. Karayiannis, Low Turbulence Natural Convection in an Air Filled Square Cavity. Part II: The Turbulence Quantities, *International Journal of Heat and Mass Transfer* 43: 867-884, 2000.

[7] F. Ampofo, T.G. Karayiannis, Experimental benchmark data for turbulent natural convection in an air filled square cavity, *International Journal of Heat and Mass Transfer* 46: 3551-3572, 2003.

[8] A.A. Dafa'Alla, P.L. Betts, Experimental study of turbulent natural convection in a tall air cavity. *Experimental Heat Transfer* 9(2): 165–194, 1996.

[9] G. Barakos, E. Mitsoulis, Natural convection flow in a square cavity revisited: laminar and turbulent models with wall functions, *International Journal for Numerical Methods in Fluid* 18**:** 695-719, 1994.

[10] F. Penot, O. Skurtys, S. Didier, Preliminary experiments on the control of natural convection in differentially–heated cavity, *International Journal of Thermal Science* 49: 1911-1919, 2010.

[11] D. Saury, R. Nicolas, F. Djana, F. Penot, Natural convection in an air-filled cavity: Experimental results at large Rayleigh numbers, *International Communications in Heat and Mass Transfer* 38: 679-687, 2011.

[12] R.G.M. Hasan, J.J. McGuirk, D.D. Apsley, A turbulence model study of separated 3D jet/afterbody flow, *AERONAUT J*, 108: 1-14, ISSN:0001-9240, 2004

[13] S.J. Wang, A.S. Mujumdar, A comparative study of five low Reynolds number $k-\varepsilon$ models for impingement heat transfer.Applied Thermal Engineering 25: 31-44, 2004.

[14] ANSYS FLUENT 12.0 (2009).

[15] Z. Yang, T.H. Shih, New time scale based k-e model for near-wall turbulence. *AIAA J.* 31: 1191-1198, 1993.

[16] R. Abid, Evaluation of two-equation turbulence models for predicting transitional flows, *International Journal of Engineering Science* 31 (6): 831–840, 1993.

[17] C.K.G. Lam, K. Bremhost, A modified form of the k–e model for prediction wall turbulence: Transactions of the ASME, *Journal of Fluids Engineering* 103: 456–460, 1981.

[18] B.E. Launder, B.I. Sharma, Application of the energy-dissipation model of turbulence to the calculation of flow near a spinning disc, *Letters in Heat and Mass Transfer* 1: 131–138, 2002.

[19] K. Abe, T. Kondoh, Y. Nagano, A new turbulence model for predicting fluid flow and heat transfer in separating and reattaching flows I: Flow field calculations, *International Journal of Heat and Mass Transfer* 37 (1): 139–151, 1994.

[20] K.C. CHANG, W.D. Hsieh, C.S Chen, A modified low-Reynolds-number turbulence model applicable to recirculating flow in pipe expansion, Transactions of the ASME, *Journal of Fluids Engineering* 117 : 417-423, 1995.